Ideal-MHD Eigenvalue Analysis of Spectral Elements

Carl Sovinec

University of Wisconsin-Madison

CEMM/NIMROD Summer Meeting

June 12-15, 2012

Madison, Wisconsin

Thesis

Ideal-MHD eigenvalue analysis of 1D and 2D spectral elements offers an improved approach to primitive-variable extended-MHD computation.

Outline

- Introduction
  - standard NIMROD implementation
  - interchange
- Improvements based on 1D analysis
  - expansion sensitive to divergence
  - penalty-method application
  - results
- Progress on 2D analysis
- Conclusions

Introduction: NIMROD's C^0 spectral-element implementation is formulated to allow dissipation for each physical field.

- Like conventional thermal-conduction and structural-mechanics applications, second-order derivatives lead to mathematical 'energy' increasing as spatial scales decrease.
  - Second-order terms get integrated by parts.
  - In 1D, for example:

$$-\frac{d^2v}{dx^2} = f \quad \Rightarrow \quad \int \frac{dw}{dx}\frac{dv}{dx}dx = \int w f \, dx \quad \text{for all } w \text{ in } H_e^1$$

  - Continuous functions are necessary and sufficient (in the sense that greater continuity is not required).
- First-order spatial derivatives do not provide a coercive energy. The following single-field formulation does not bound fine-scale oscillations.

$$-\frac{dv}{dx} = \frac{dv}{dt} \quad \Rightarrow \quad -\int w \frac{dv}{dx} dx = \int w \frac{dv}{dt} dx \quad \text{for all } w \text{ in } H_e^1$$

- *The extended-MHD dilemma is that physical dissipation is important but small, and there are sources of energy at small scales.*

Local interchange drives small spatial scales, and the physical bending energy is critical.

• With local MHD interchange, the physically stabilizing contribution is singular mathematically, and the drive is local. In normalized reduced ideal MHD:

$$\frac{\partial}{\partial x}\left[\left(\omega^2 - x^2\right)\frac{\partial}{\partial x}\Phi\right] - D_s\Phi = 0$$

destabilizing interchange

inertia

stabilizing bending from the singular $\mathbf{B}\cdot\nabla(\mathbf{B}\cdot\nabla\Phi)$

Φ is the streamfunction, *x* is flux-normal distance from the resonance, and ω is frequency.

• Analytically, all eigenvalues σ of $-\frac{\partial}{\partial x}x^2\frac{\partial}{\partial x}\Phi$ for oscillatory solutions satisfy σ > 1/4.

- D_s > 1/4 allows $\omega^2 < 0$, i.e. instability.

• In extended-MHD equations, bending is represented by first-order derivatives in separate equations.

With non-reduced, primitive-variable equations, several numerical operations have to work well together *at the limit of resolution* to produce the stabilizing effect.

- A relatively simple example is compressible *g*-mode analysis with mass density increasing in *y*, supported by $J_z B_x$.

$$\frac{\partial}{\partial y}\left[\left(\frac{AS}{k^2 S-\rho^2\omega^4}\right)\frac{\partial}{\partial y}\xi_y-\rho\omega^2 J_z B_x A\xi_y\right]-\left(A+\frac{\rho g}{L}\right)\xi_y=0$$

A in numerator is from **B**·∇**b** & **B**·∇ξ.

Substitute continuity into *y*-comp of momentum eqn.

Denominator & *y*-derivs are from eliminating ∇·ξ with total pressure and different comps of momentum equation.

$$A\equiv\rho\omega^2-F^2\quad;\quad F\equiv\mathbf{k}\cdot\mathbf{B}=k_x B_x+k_z B_z\sim x^2\quad(\text{Alfven spectrum is }A=0.)$$

$$S\equiv\rho\omega^2\left(B^2+\gamma P\right)-F^2\gamma P\quad(\text{'sound' spectrum is }S=0.)$$

- Numerical response to divergence of flow at small scales is important.

NIMROD's standard spectral-element representation with diffusive $\nabla\cdot\mathbf{B}$ control and equal-order **V**, **B**, and *p* expansions converges from the unstable side.

• Test case is m=4, k=-1.78 Suydam mode at r_s=0.371 and $D_s(r_s)$=0.443.

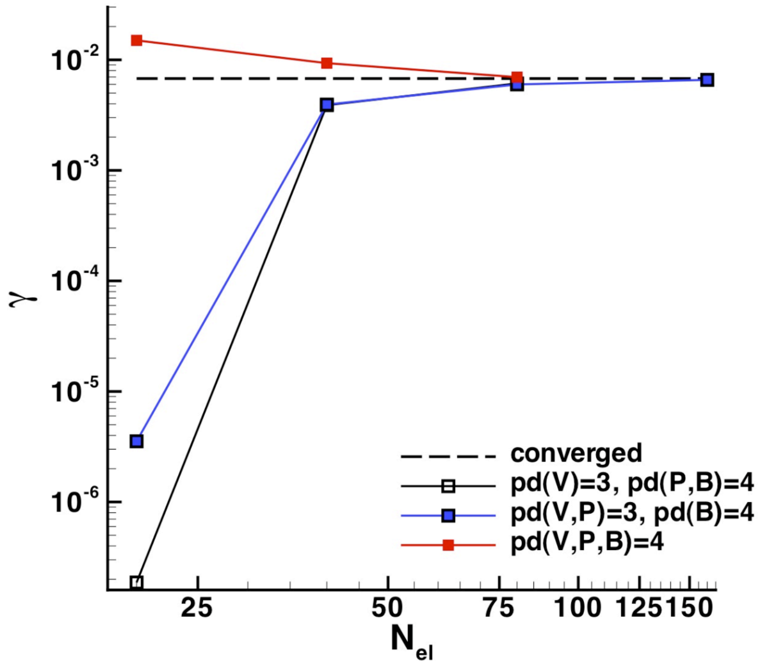

CYL_SPEC 1D eigenvalue results compare different expansions.

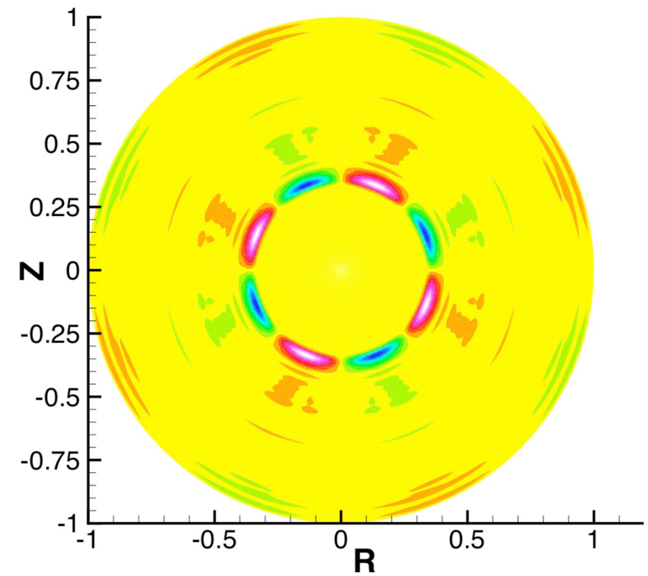

NIMROD with pd(V) reduced also converges from stable side.

• Expansions with **B** having larger polynomial degree than other fields is a generalization of the XTOR approach. [Lütjens and Luciani, CPC **95**]

• However, just reducing the polynomial degree for **V** admits numerical 0-frequency modes at mesh scales that accumulate in nonlinear computations.

Improvements based on 1D Analysis: First, use vector/scalar combinations that are sensitive to divergence on all scales.

- Arranging all contributions to $\nabla\cdot\mathbf{V}$ to be in the same space as p ensures sensitivity to divergence.
  - With q^* being the test function for p, the integrated $\nabla\cdot\mathbf{V}$ term is

$$\int q^* \nabla \cdot \mathbf{V} dVol = 2\pi L_z \int q^* \left[\underline{\frac{d}{dr}\left(rV_r\right) - imV_\theta - ik\left(rV_z\right)} \right] dr$$

i.e. $\frac{\partial}{\partial u_i}\left(J\mathbf{V}\cdot\nabla u_i\right)$

  - If the expansion for rV_r is one order greater than those for V_θ, rV_z, and q^* with a discontinuous expansion for q^* (and p), the pressure equation is sensitive to $\nabla\cdot\mathbf{V}$ at all scales.
  - All of these $J\mathbf{V}\cdot\nabla u_i$ components can be continuous.
- Hyperbolic divergence control for **B** with an auxiliary scalar ϕ is analogous to neutral-fluid acoustics (p,**V**) and avoids artificial resistive diffusion.

$$\frac{\partial}{\partial t}\mathbf{B} = -\nabla \times \mathbf{E} - \nabla\phi$$

$$\frac{\partial}{\partial t}\phi = -c_b^2 \nabla \cdot \mathbf{B}$$

Second, include a numerical term to assist the physical bending energy.

• Degtyarev and Medvedev (CPC **43**) proposes and analyzes a numerical penalty energy for low-order hybrid finite elements.

  • Hybrids use more than one expansion for the same physical quantity.

  • They are accurate, but individual tent functions can generate numerically growing modes at D_s<1/4.

• Their 'auxiliary' eigenvalue problem demonstrates numerical bending responses.

$$\frac{d}{dx}\left(x^2 \frac{d}{dx} u\right) + \lambda u = 0 \, , \quad u(\pm\varepsilon) = 0$$

In the appropriate Hilbert space,

$$\frac{a(u,u)}{b(u,u)} \geq 1/4$$

$$a(u,v) \equiv \int_{-\varepsilon}^{\varepsilon} x^2 u' v' dx \quad , \quad b(u,v) \equiv \int_{-\varepsilon}^{\varepsilon} uv dx \quad , \quad u' \equiv du/dx$$

Their numerical penalty compensates the hybrid shortcomings.

- Degtyarev applies the following relation for piecewise linear expansion

$$\int \bar{c} u v \, dx = \int \bar{c}\,\bar{u}\,\bar{v} \, dx + \frac{h^2}{12} \int \bar{c} u' v' \, dx$$

to show that the numerical form of the auxiliary problem is

$$a_h(u,v) \equiv \int_{-\varepsilon}^{\varepsilon} x^2 u' v' dx - \alpha h^2 \int_{-\varepsilon}^{\varepsilon} u' v' dx$$

$$b_h(u,v) \equiv \int_{-\varepsilon}^{\varepsilon} u v dx - \beta h^2 \int_{-\varepsilon}^{\varepsilon} u' v' dx$$

where α and β depend on the hybrid formulation,

$$\frac{a_h(u,u)}{b_h(u,u)} \geq \frac{1}{4} + \frac{A}{4(1-\beta A)(1-A/12)}\left[\frac{A}{16} + \Delta\left(1 - \frac{A}{12}\right)\right] \qquad A \equiv h^2 \int_{-\varepsilon}^{\varepsilon} (u')^2 dx \Bigg/ \int_{-\varepsilon}^{\varepsilon} u^2 dx$$

and $\Delta \equiv \frac{3}{4} - 4\alpha + \beta \geq 0$ is sufficient to avoid numerical destabilization.

- Adding a numerical penalty energy $\propto h^2 \int_{-\varepsilon}^{\varepsilon} (u')^2 dx$ to $a_h(u,u)$ can be used to compensate destabilization in hybrid formulations with Δ<0.

The numerical penalty energy can be adapted to our first-order-in-time equations.

• Including numerical terms with second-order spatial derivatives would amount to damping, which we would like to avoid.

• A numerical response to parallel vorticity can be ensured with another scalar:

$$\rho \frac{\partial}{\partial t}\mathbf{V} \rightarrow -i\omega\rho\mathbf{V} = \mathbf{F} + \hat{\mathbf{b}} \times \nabla\lambda$$

$$\frac{\partial}{\partial t}\lambda \rightarrow -i\omega\lambda = c_\lambda^2 \hat{\mathbf{b}} \cdot \nabla \times \mathbf{V}$$

• Combining and incorporating the penalty in the reduced-MHD streamfunction equation indicates its effect:

$$\frac{\partial}{\partial x}\left[\left(\omega^2 - x^2\right)\frac{\partial}{\partial x}\Phi\right] - D_s\Phi + c_\lambda^2 \frac{\partial^4}{\partial x^4}\Phi = 0$$

• If the λ-expansion in each element has just last orthogonal polynomial of the expansion for velocity, it only penalizes oscillation at the smallest spatial scales of a given mesh.

1D eigenvalue results for m=1 waves in a uniform-**B**, $\beta=\Gamma=1$ cylinder show that the new $J\mathbf{A}\cdot\nabla u_i$ representation avoids spectral pollution.

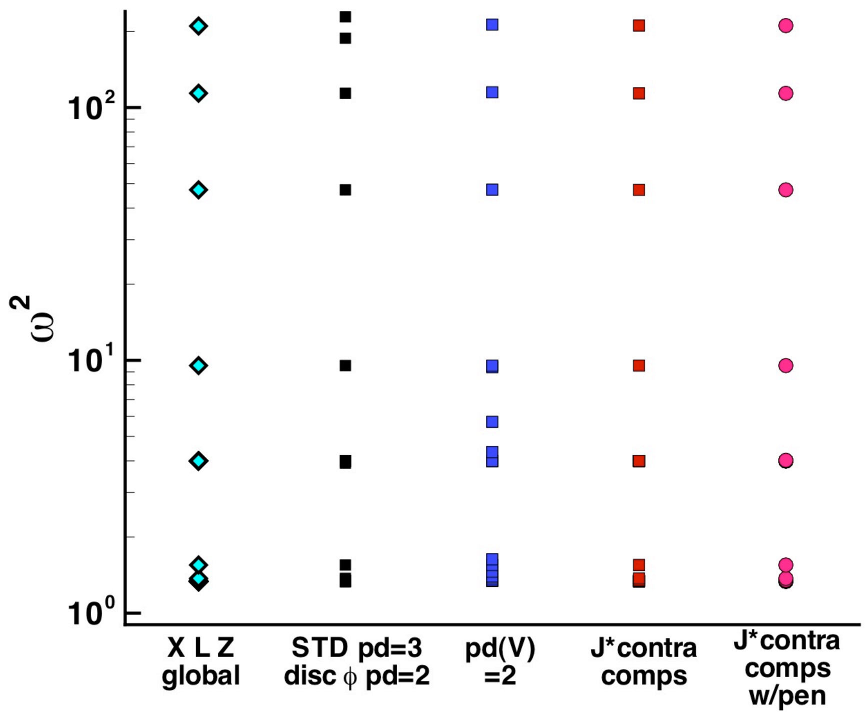

The 'XLZ' results are computed with global Chebyshev polynomials and are accurate.

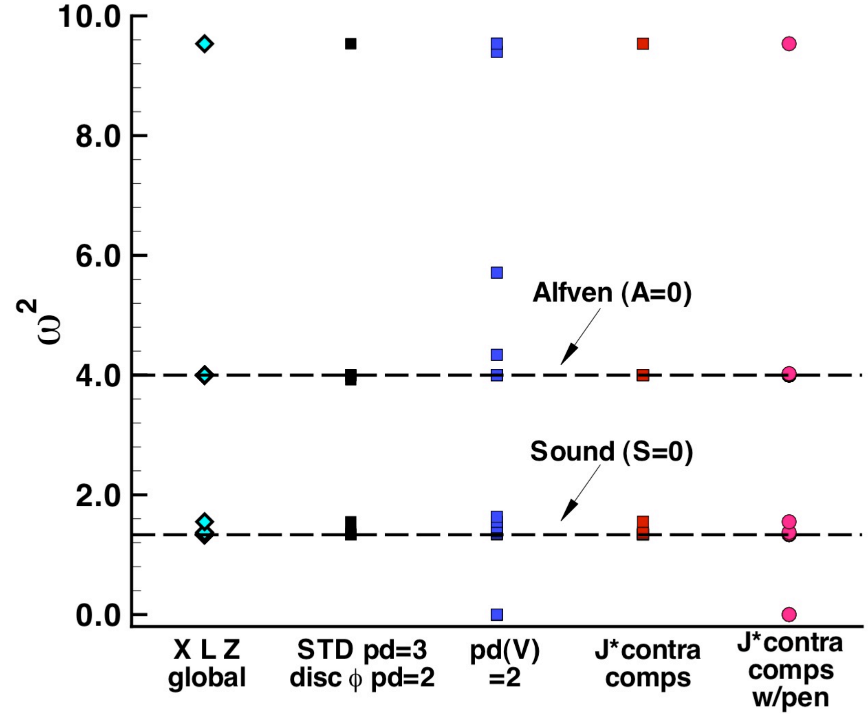

This linear-scale plot shows critical low-frequency behavior.

- The reduced-**V** expansion has zero-frequency modes and spectral pollution.
- Modes of the new $J\mathbf{A}\cdot\nabla u_i$ representation are close to the XLZ results.

The penalty adds one 0-frequency mode per element to the $J\mathbf{A}\cdot\nabla u_i$ representation.

- Unlike results with the reduced-**V** representation, these modes are essentially orthogonal to the physical fields.

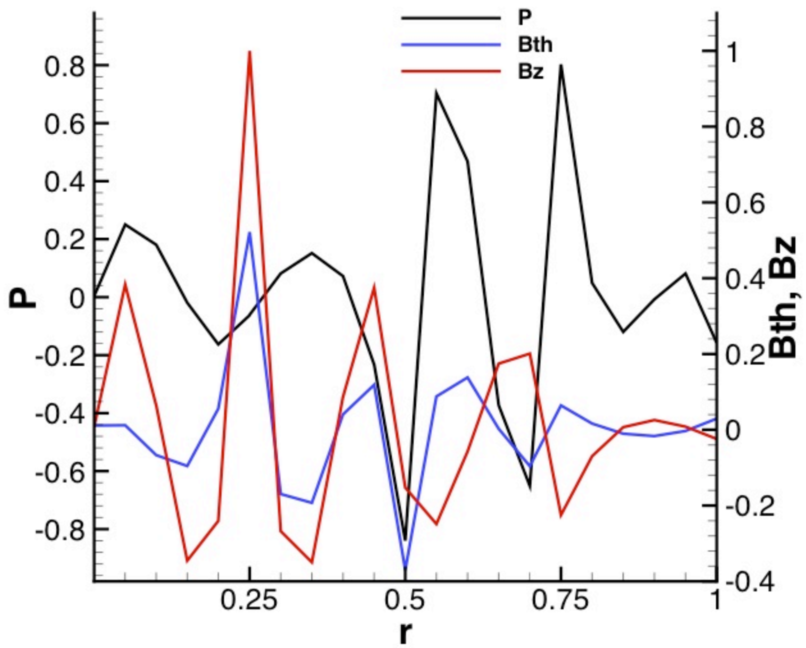

Physical-field components of a 0-frequency mode with reduced-V are O(1).

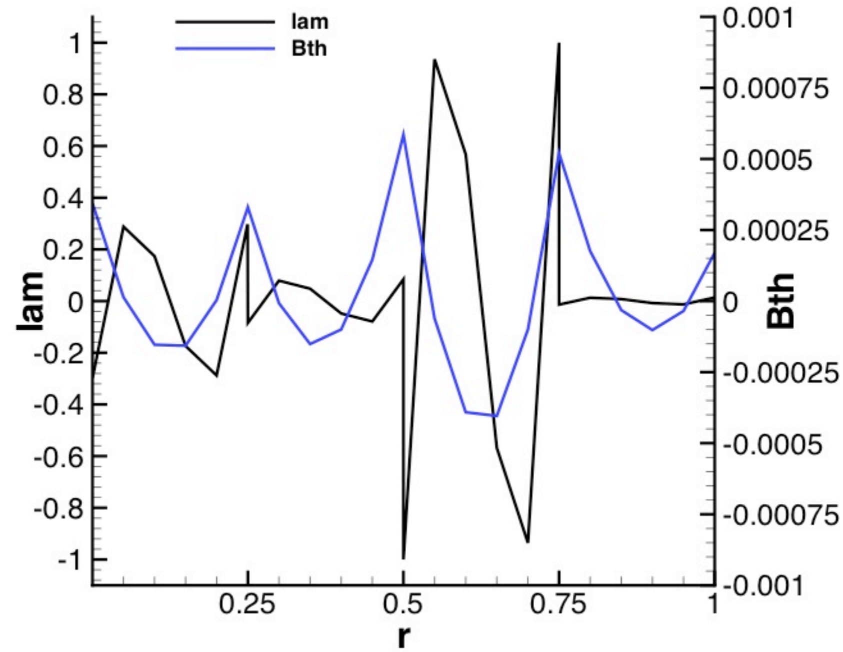

0-frequency modes with the new representation are essentially λ-only. [Penalty equation is insensitive to $\nabla_{||}\lambda$.]

- Nonlinear terms in extended-MHD computation will not project onto the 0-frequency modes in the new representation. [Recall $\partial\lambda/\partial t = c_\lambda^2 \hat{\mathbf{b}}\cdot\nabla\times\mathbf{V}$.]

Results from a physically stable Suydam test, run with hyperbolic $\nabla\cdot\mathbf{B}$ control, show no numerical destabilization with either reduced-**V** or with $J\mathbf{A}\cdot\nabla u_i$ + penalty.

- This test case has β=14%, m=4, k=-1.5, r_s=0.507 and $D_s(r_s)$=0.200.
- Results with reduced-**V** and $J\mathbf{A}\cdot\nabla u_i$+penalty are not plotted (γ=0).

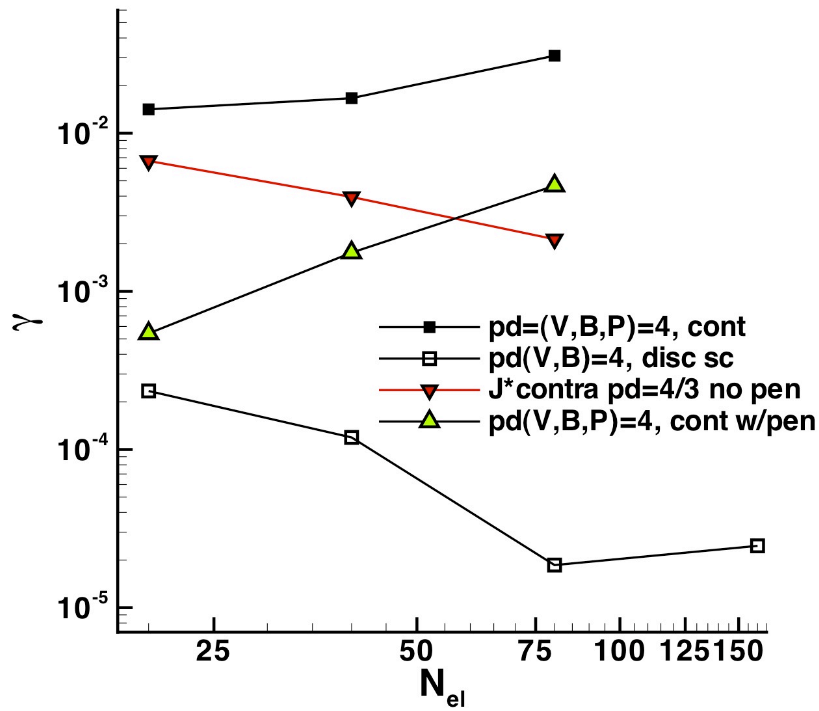

- The red-gradient and yellow-delta traces show that neither $J\mathbf{A}\cdot\nabla u_i$ alone nor the penalty alone is sufficient.
- The representation of the open-rectangle trace is analogous to FE application to Stokes flow.

A physically unstable case shows that $J\mathbf{A}\cdot\nabla u_i$ + penalty converges to the Suydam mode when the λ-representation is just the largest Legendre polynomial.

- This test case has m=4, k=-1.78, r_s=0.371 and $D_s(r_s)$=0.443.

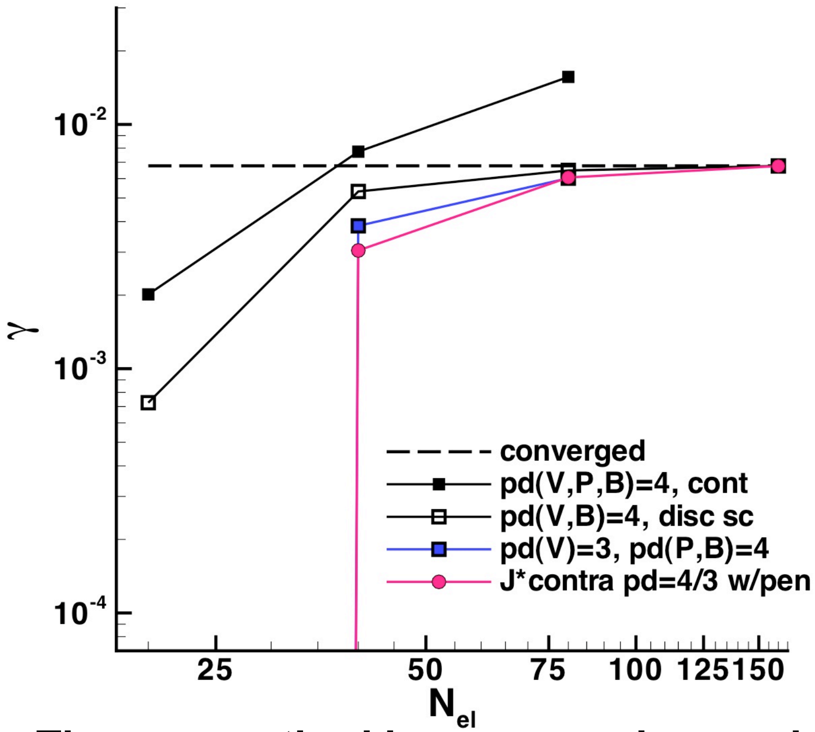

The new method has no growing modes with 20 elements.

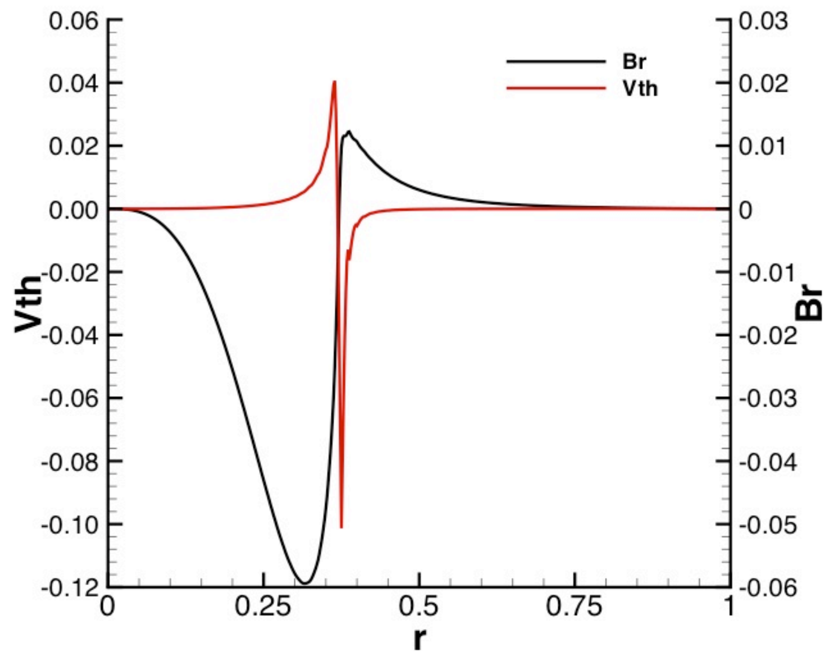

Components of the unstable mode from the 80-element, $J\mathbf{A}\cdot\nabla u_i$ + penalty computation.

- If the λ-representation is complete (not just last polynomial), the $J\mathbf{A}\cdot\nabla u_i$ expansion with the same $c_\lambda^2 = 1\times 10^{-4}$ does not reproduce the physical mode.

Summarizing properties and 1D results for the $J\mathbf{A}\cdot\nabla u_i$ + penalty method …

- Vector components are continuous, which allows dissipation in extended-MHD computation.
    - Dissipation for scalars will need flux vectors, but all scalars are eliminated from matrices prior to external linear solves.
- The only 0-frequency modes are essentially λ-only (1 per element).
- Physically stable cases show no numerical destabilization.
- Physically unstable cases converge from the stable side.
- Overstable modes have not been produced any of the tests.
- Penalizing just the highest-order polynomial implies that results are not critically sensitive to the choice of the c_λ^2 coefficient.

Progress on 2D analysis: Many requirements for a 2D spectral-element implementation of the new method have been developed.

- The first step is recognizing the different nodal meshes in an element.

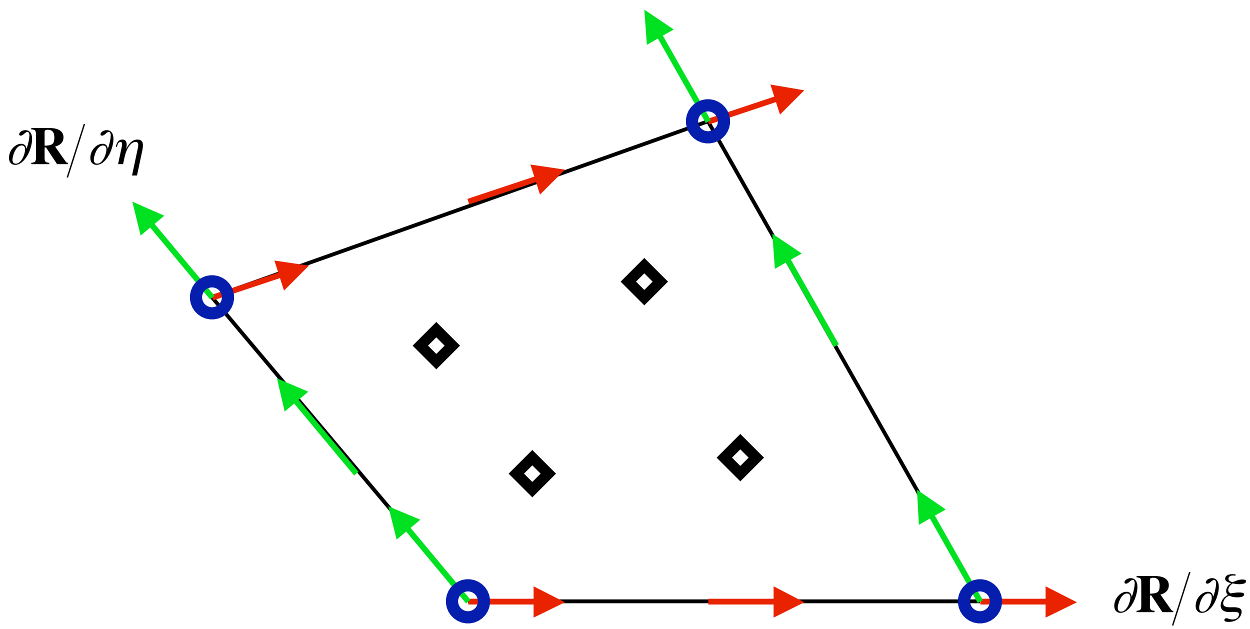

- This sketch of a lowest-order biquadratic/bilinear element shows basis vectors at their node locations.
    - Circles are locations of continuous perpendicular components ($\partial\mathbf{R}/\partial\phi$).
    - Diamonds are nodes of scalars (discontinuous nodal), or scalars may have modal expansions that have no nodes.

Generalizing the method from 1D, physical vectors are continuous across element borders (approximately, at least).

• Along the common edge between adjacent elements, each of

$$\partial\mathbf{R}/\partial u_{\text{tang}} \quad \text{and} \quad \partial\mathbf{R}/\partial u_{\text{tang}} \times \partial\mathbf{R}/\partial\phi \quad (\parallel \text{ to } \nabla u_{\text{norm}} \text{ not } \partial\mathbf{R}/\partial u_{\text{norm}})$$

are unique and may be used to relate the native $J\mathbf{A}\cdot\nabla u_i$ components.

• With curved elements, there will be high-order discontinuities between node locations.

• Indirect addressing between element degrees of freedom (DOF) and global DOF simplifies matrix construction, even with structured collections of elements.

   • Unstructured blocks of quadrilaterals are tractable.

NIMEIG is an implementation to test the new 2D spectral-el. / 1D Fourier bases prior to time-dependent computation.

- Mesh generation for structured arrangements of quadrilaterals has been developed.
- Data structures and mathematical operators have been developed for the new vector expansion and for continuous and discontinuous scalars.
- A routine to map element DOF to global algebraic-system (matrix) components has been implemented.
- Simplified PDE systems have been implemented for benchmarking:
    - Second-order in time scalar wave equation (one dependent field).
    - First-order acoustic wave equation (p, $\mathbf{V}$).
    - First-order ideal MHD with uniform background $\mathbf{B}$.
- Like CYL_SPEC, NIMEIG uses LAPACK to solve the eigenmode problems.

Initial results from the uniform-**B** implementation indicate the state of development.

- Computations are in a periodic cylinder with a=1, L_z=2π/7, β=Γ=1.
- The 2D mesh is used for the *r*-*z* plane and *m*=1. (4×2, poly. deg.=3/2)

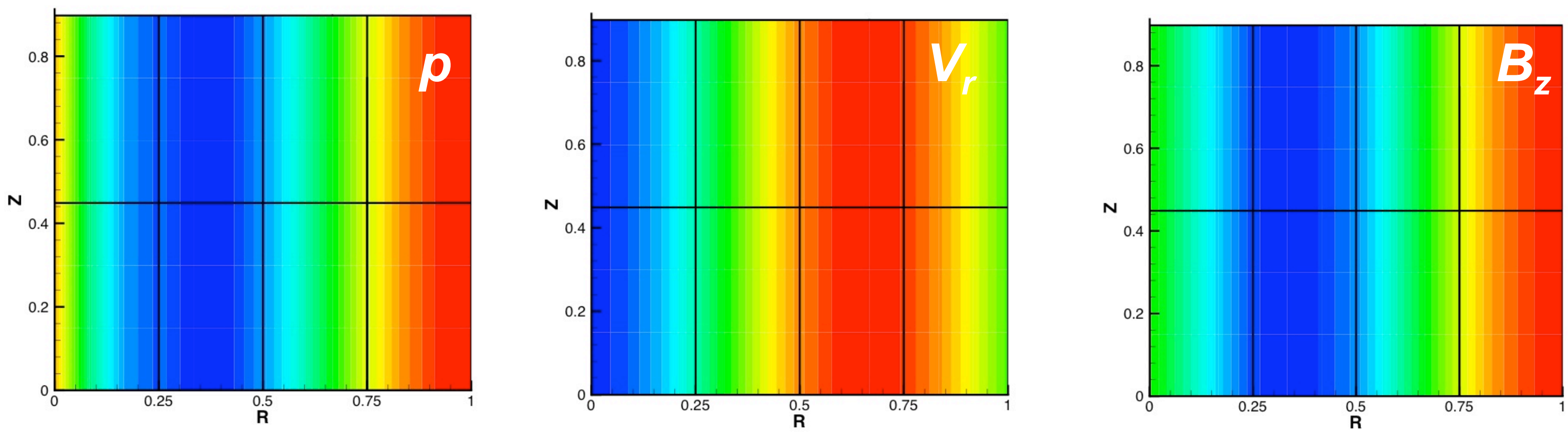

The second *k*=0 fast mode has $\omega_{analytic}$=6.529. NIMEIG: ω=6.528.

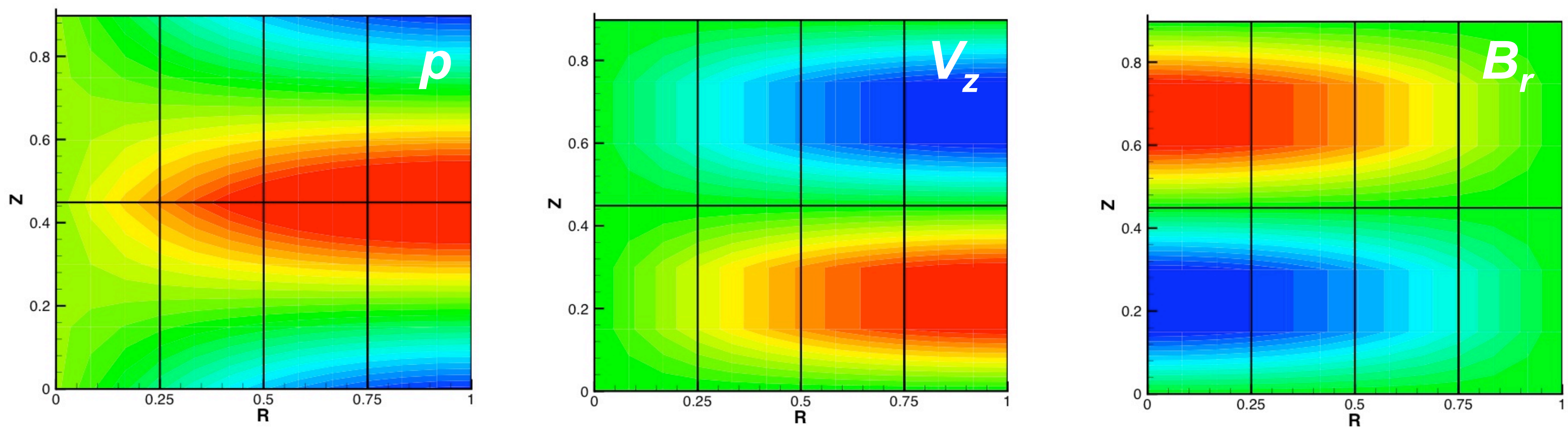

The fastest *k*=7 slow mode has $\omega_{analytic}$=4.812. NIMEIG: ω=4.845.

Benchmarking NIMEIG spectra and checking for numerical modes is beginning.

Spectra from NIMEIG have a lot of information.

• All k represented by a mesh / element choice are included.

  • Identifying spectral pollution is much more difficult.

  • Segregation of modes by a transform in z would help.

• The periodic system admits correct 0-frequency modes.

• With high-order finite elements, the same physical mode shifted in phase by less than $k\Delta z/2$ produces slightly different numerical eigenvalues.

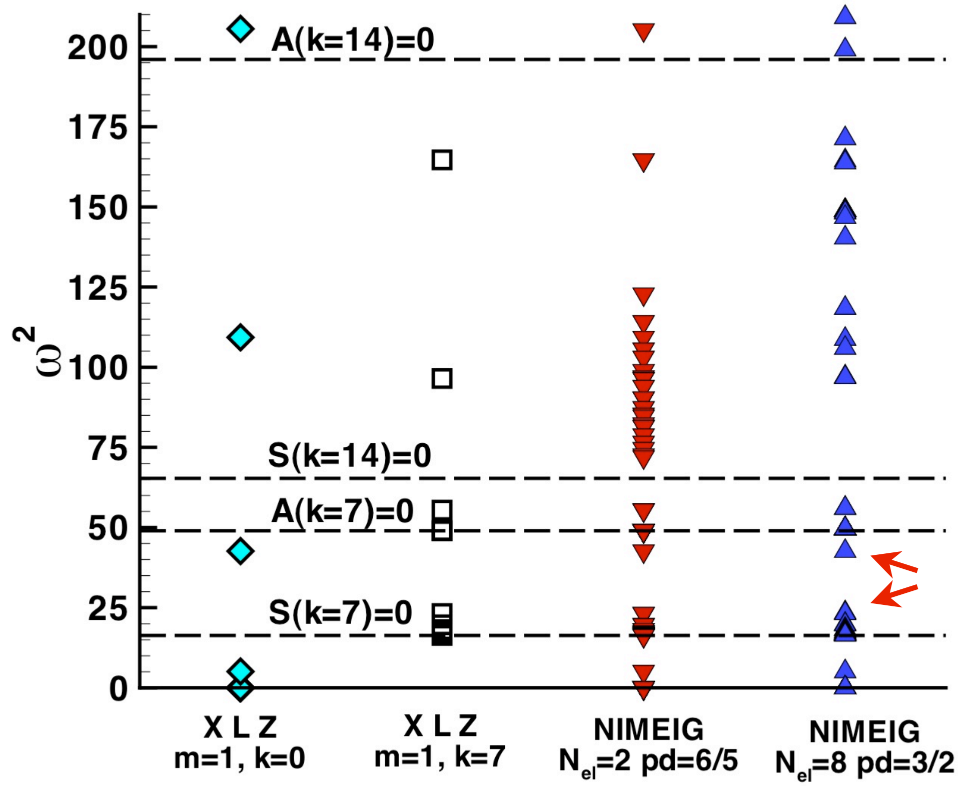

Comparison of two m=1 CYL_SPEC spectra (k=0 and k=7) and two m=1 NIMEIG spectra (all k): 2×1, degree 6/5; and 4×2, degree 3/2.

Arrows indicate modes shown on previous slide.

Next steps with NIMEIG include …

- Checking for unphysical 0-frequency modes and spectral pollution in uniform-**B** conditions
    - Post-processing to separate different *k*-values is needed
- Incorporating the complete ideal-MHD system for nontrivial equilibria and the parallel-vorticity penalty equation
- Completing the element-to-global matrix relations for changes in basis vectors between adjacent elements
- Coupling to SCALAPACK or other parallel eigenvalue solvers for larger systems
- Technology transfer to NIMROD if or when results are sufficiently promising

Conclusions

- Avoiding numerical ideal-MHD destabilization with spectral elements requires attention to flow-divergence and bending.

- 1D eigenmode analysis (CYL_SPEC) shows no numerical destabilization from the new mixed-degree $J\mathbf{A}\cdot\nabla u_i$ expansion with parallel-vorticity penalty and hyperbolic $\nabla\cdot\mathbf{B}$ control.

    - A number of other methods including reduced continuous **V**, discontinuous lower-order scalars, and finite-element "stabilization" methods have not avoided numerical destabilization without introducing 0-frequency modes.

- NIMEIG is being developed for testing 2D elements for NIMROD and may become a production eigenmode solver.

CYL_SPEC is being used to investigate many possible expansions and formulations.

• 1D cylindrical geometry with $f \rightarrow f(r)e^{im\theta+ikz}$ is a compromise between non-trivial geometry and rapid development.

• Run-time parameters are used to select basis functions.

  • Basis functions in *r* may be continuous and discontinuous spectral elements of arbitrary polynomial degree.

  • Basis vectors are orthogonal, and the two for the θ-*z* plane may rotate in *r* to follow $\mathbf{B}_0$: $\left(\hat{\mathbf{r}}, \hat{\mathbf{b}} \times \hat{\mathbf{r}}, \hat{\mathbf{b}}\right)$.

• Changing formulations requires minimal coding.

• Three configurations are considered: 1) uniform B_z to check stable waves, 2&3) a peaked-pressure profile where D_s decreases monotonically in radius, and *m*=4 is stable/unstable depending on k_z.

  • Modes resonant outside *r* = 0.466 are stable.

  • For k_z=-1.5, r_s=0.507, and D_s=0.200; for k_z=-1.78, r_s=0.371, and D_s=0.443.

$$B_z(r) = B_0 \qquad q(r) = \frac{1 + c_2^2 r^2}{R c_1} \qquad D_s(r) = -\frac{\mu_0}{r B_z}\left(\frac{q}{dq/dr}\right)^2 \left(\frac{dP}{dr}\right) = \frac{c_1^2}{\left(1 + c_2^2 r^2\right) c_2^4 r^2}$$